Available online at www.sciencedirect.com
ScienceDirect
Solar Energy Materials & Solar Cells 91 (2007) 1652–1657
Solar Energy Materials and Solar Cells
www.elsevier.com/locate/solmat

Analytical model of mismatched photovoltaic fields by means of Lambert W-function

G. Petrone[a], G. Spagnuolo[a,*], M. Vitelli[b]

[a]DIIIE, Università di Salerno, Via Ponte Don Melillo, Fisciano (SA), Italy
[b]DII, Seconda Università di Napoli, Real Casa dell'Annunziata, Aversa (CE), Italy

Received 1 December 2006; received in revised form 10 May 2007; accepted 11 May 2007
Available online 3 July 2007

Abstract

A new model of photovoltaic (PV) fields is introduced in this paper. It allows the simulation of a PV generator whose subsections, e.g. cells, groups of cells, panels or group of panels, work under different solar irradiation values and/or at different temperatures. Moreover, different nominal characteristics, rated power, production technology, shape and area can be settled for different subsections. Consequently, the proposed model is able to describe the behaviour of matched as well as mismatched PV fields. It results into a non linear system of equations, which includes bypass and blocking diodes models and is characterized by a sparse Jacobian matrix. The numerical model is reliable and requires a moderate computational burdensome, both in terms of memory use and processor speed. Numeric simulations confirm the accuracy and cheapness of the approach. The proposed model is used to simulate the drawbacks associated to mismatching during maximum power point tracking (MPPT) of the PV generator.

Keywords: Lambert W-function; Solar cell array

1. Introduction

In order to draw the maximum power from a photovoltaic (PV) field at the current solar irradiance level and temperature, it is mandatory to match the PV source with the load by means of a switching DC–DC converter. Its duty cycle must be controlled by means of a maximum power point tracking (MPPT) strategy, which must be suitable to ensure the source-load matching by properly changing the operating voltage at the PV array terminals in function of the actual weather conditions. Any efficient MPPT technique must be able to detect the voltage value corresponding to the maximum power that can be delivered by the PV source.

Most of the MPPT strategies, e.g. perturb and observe (P & O) and incremental conductance (IC) methods, properly work in presence of a uniform irradiance of the PV array, since they are able, although by means of different processes, to detect the unique peak of the power versus voltage characteristic of the PV array. Unfortunately, in many real cases, the PV field does not receive a uniform irradiation and/or not all its parts (panels as well as single cells) work at the same temperature, so that mismatches among different parts of the array may arise. Simulation results as well as experimental measurements presented in the literature (see for example Refs. [1–5]) have put in evidence the detrimental effect of mismatching conditions on the energy production of the PV power plant.

To relieve the power drop caused by a mismatch, a bypass diode is used in anti-parallel with each PV basic unit, e.g. a panel. A blocking diode is placed in series with each totem of PV basic units connected in series. This

*Corresponding author. Tel.: +39 089 964 258; fax: +39 089 964 218.
E-mail addresses: gpetrone@unisa.it (G. Petrone), spanish@ieee.org (G. Spagnuolo), vitelli@unina.it (M. Vitelli).

0927-0248/$ - see front matter
doi:10.1016/j.solmat.2007.05.021

precaution increases the plant cost, but avoids that a basic PV unit or a series of them absorbs the current produced by others.

Whenever a mismatch occurs, any technique has a high probability to fail the MPPT goal, since the PV characteristic may exhibit more than one peak, with one absolute maximum power point and one or more points of relative maximum power. In this case, standard MPPT techniques are likely deceived and consequently they track a point where $\mathrm{d}P/\mathrm{d}v = 0$, but that is not the maximum power point.

In order to design a robust MPPT strategy, which must be effective both in homogeneous as well as mismatched working conditions, an accurate and reliable numerical model of the PV field is mandatory.

This paper introduces a model of PV fields that allows to simulate mismatched conditions in both general purpose and circuit-oriented environments. It is based on the use of Lambert W-function [6], which has been fruitfully used to the aim of expressing the current–voltage characteristic of a solar array.

The paper is organised as follows: Section 2 shows the details of the proposed model and puts in evidence its features. Section 3 shows the results of some application examples and puts in evidence the need of a suitable MPPT controller if mismatching conditions arise, and Section 4 is devoted to conclusions and hints for future work.

2. The model

In Fig. 1 the usual circuit model of a PV panel is shown. Such a model recurs very often in the literature (e.g. in Refs. [7–9]). It includes the light induced current generator I_{ph} and series and shunt resistances R_{s} and R_{h}, respectively; D_{b} is the bypass diode. We suppose, without loss of generality, that one bypass diode is placed in anti-parallel with the whole panel.

The relation between the PV generator current I and voltage V is evaluated by solving the following system of non linear equations:

$$I_{\mathrm{d}} = I_{\mathrm{sat,d}}(\mathrm{e}^{V_{\mathrm{d}}/V_{t,\mathrm{d}}} - 1), \tag{1}$$

$$I_{\mathrm{db}} = I_{\mathrm{sat,db}}(\mathrm{e}^{-V/V_{t,\mathrm{db}}} - 1), \tag{2}$$

$$I = I_{\mathrm{db}} + I_{\mathrm{ph}} - I_{\mathrm{d}} - I_{\mathrm{h}}, \tag{3}$$

$$V_{\mathrm{d}} = V + R_{\mathrm{s}}I_{\mathrm{s}} = V + R_{\mathrm{s}}(I - I_{\mathrm{db}}), \tag{4}$$

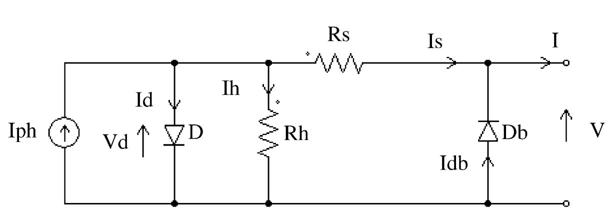

Fig. 1. Circuit model of a PV panel including the bypass diode Db.

$$I_{\mathrm{h}} = \frac{V_{\mathrm{d}}}{R_{\mathrm{h}}} = \frac{V + R_{\mathrm{s}}(I - I_{\mathrm{db}})}{R_{\mathrm{h}}}. \tag{5}$$

Such a system has been obtained by using Kirchhoff voltage and current laws, namely Eqs. (3) and (4), Ohm laws for shunt and series resistors, namely Eqs. (4) and (5), and non linear Eqs. (1) and (2) for the diode D included in the model of the panel and for the bypass diode Db, respectively. In Eq. (1) $V_{t,\mathrm{d}} = \eta_{\mathrm{d}} V_{T,\mathrm{d}}$ and in Eq. (2) $V_{t,\mathrm{db}} = \eta_{\mathrm{db}} V_{T,\mathrm{db}}$, $V_{t,\mathrm{d}}$ and $V_{t,\mathrm{db}}$ are expressed as the product of the diode ideality factor and the thermal voltage. The latter, as well as the two saturation currents $I_{\mathrm{sat,d}}$ and $I_{\mathrm{sat,db}}$, depends on temperature T only, whereas the light induced current I_{ph} depends on the irradiance level S and on the array temperature T [8].

The system of Eqs. (1)–(5) clearly shows that the PV array current I is a non linear and implicit function of the PV array voltage V, of the irradiance level S and of the temperature T. Nevertheless, such a non linear system can be symbolically solved in one of the actually available symbolic calculation environments, such as Matlab® and Mathematica®. In this way, a non linear relationship between the current I and the voltage V at the basic PV unit terminals can be obtained. Such relationship is reported in Eq. (6): it makes use of the Lambert W-function of the term θ whose value depends on the terminal voltage V and is reported in Eq. (7).

$$I = \frac{[R_{\mathrm{h}}(I_{\mathrm{ph}} + I_{\mathrm{sat,d}}) - V]}{(R_{\mathrm{h}} + R_{\mathrm{s}})} + I_{\mathrm{sat,db}}(\mathrm{e}^{-V/V_{t,\mathrm{db}}} - 1) - \frac{V_{t,\mathrm{d}}}{R_{\mathrm{s}}}\,\mathrm{Lambert\,W}(\theta), \tag{6}$$

$$\theta = \frac{(R_{\mathrm{h}}//R_{\mathrm{s}})I_{\mathrm{sat,d}}\mathrm{e}^{[R_{\mathrm{h}}R_{\mathrm{s}}(I_{\mathrm{ph}}+I_{\mathrm{sat,d}})+R_{\mathrm{h}}V/V_{t,\mathrm{d}}(R_{\mathrm{h}}+R_{\mathrm{s}})]}}{V_{t,\mathrm{d}}}. \tag{7}$$

It is well known [6] that the LambertW function of the variable θ, herein indicated as LambertW(θ), is a non linear function of θ and it is the inverse function of

$$f(\theta) = \theta\,\mathrm{e}^{\theta}. \tag{8}$$

Note that the use of the Lambert W-function allows the apparently explicit calculation of the array current as a non linear function of the terminal voltage. The value of the Lambert function, for an assigned value of the independent variable θ, is efficiently provided in simulation environments such as Matlab® and Mathematica®.

Expression (6), together with well-known Lambert W-function properties, allows to calculate the first derivative of the panel's current with respect to the terminal voltage, again in apparently explicit form. In Eq. (9) it has been reported the property expressing the derivative of the LambertW(θ) function with respect to θ, and in Eq. (10)

the expression of the derivative of I with respect to V at the panel's terminals is given. In this way, the differential conductance of the panel is explicitly expressed as a function of the panel's voltage V only, by means of a non linear function.

$$\frac{\mathrm{d}}{\mathrm{d}\theta}\mathrm{Lambert\,W}(\theta) = \frac{1}{[1+\mathrm{Lambert\,W}(\theta)]\mathrm{e}^{\mathrm{Lambert\,W}(\theta)}} = \frac{\mathrm{Lambert\,W}(\theta)}{[1+\mathrm{Lambert\,W}(\theta)]\theta}, \tag{9}$$

$$\frac{\mathrm{d}I}{\mathrm{d}V} = -\frac{1}{(R_\mathrm{h}+R_\mathrm{s})} - \frac{I_{\mathrm{sat,db}}}{V_{t,\mathrm{db}}}\mathrm{e}^{-V/V_{t,\mathrm{db}}} - \frac{R_\mathrm{h}}{R_\mathrm{s}(R_\mathrm{h}+R_\mathrm{s})}\mathrm{Lambert\,W}(\theta). \tag{10}$$

Thus, in this way, both the PV current and its derivative with respect to the PV voltage have been expressed in closed form as functions of the sole voltage.

This greatly helps in formalizing the non linear algebraic system that describes a PV field composed by an arbitrary number of panels, which can be connected both in series and in parallel.

In order to explain this concept, let us refer to a string of PV panels connected in series. Fig. 2 shows the string of N series-connected panels and the blocking diode that avoids current backflows.

The model results into a system of $(N+1)$ equations in the same number of unknowns $\{V_1, V_2, \ldots, V_k, \ldots, V_{N-1}, V_N, \mathrm{V}_{\mathrm{diode}}\}$. It is enough to write one Kirchhoff voltage law and N Kirchhoff current laws. The topological constraints are formalized in Eq. (11); they can be matched with the N equations of the panels, expressed as in Eq. (6) in terms of $I_k = I_k(V_k)$, $k = 1,2,\ldots,N$, and with the characteristic equation, having the same expression of Eq. (1) of the blocking diode, thus taking into account the dependency of such a characteristic equation from the physical parameters of the real diode used.

$$\begin{cases} V_1 + V_2 + \ldots + V_k + \ldots + V_{N-1} + V_N + V_{\mathrm{diode}} - V = 0 \\ I_1(V_1) - I_2(V_2) = 0 \\ I_1(V_1) - I_3(V_3) = 0 \\ \quad\ldots \\ I_1(V_1) - I_k(V_k) = 0 \\ \quad\ldots \\ I_1(V_1) - I_{N-1}(V_{N-1}) = 0 \\ I_1(V_1) - I_N(V_N) = 0 \\ I_1(V_1) - I_{\mathrm{diode}}(V_{\mathrm{diode}}) = 0 \end{cases} . \tag{11}$$

The non linear system (11) includes N non linear equations and one linear equation, the first one, in which the terminal voltage V, that is assumed to be a known term, appears. Each non linear equation includes only two of the $(N+1)$ unknowns, and the first one is always V_1. This choice has been made to simplify the expression of the Jacobian matrix needed to solve the non linear system by means of, for example, the Newton Raphson method.

Thanks to Eq. (10) it is possible to obtain each term of the Jacobian matrix J as a function of the unknowns. Moreover, the structure of the system has been properly chosen in order to simplify the structure of the Jacobian matrix that, as it is well known, needs to be inverted when using Newton Raphson iterative methods. The Jacobian matrix structure is reported in Eq. (12) which puts in evidence that it is sparse and with a pattern which is characteristic of doubly bordered and diagonal square

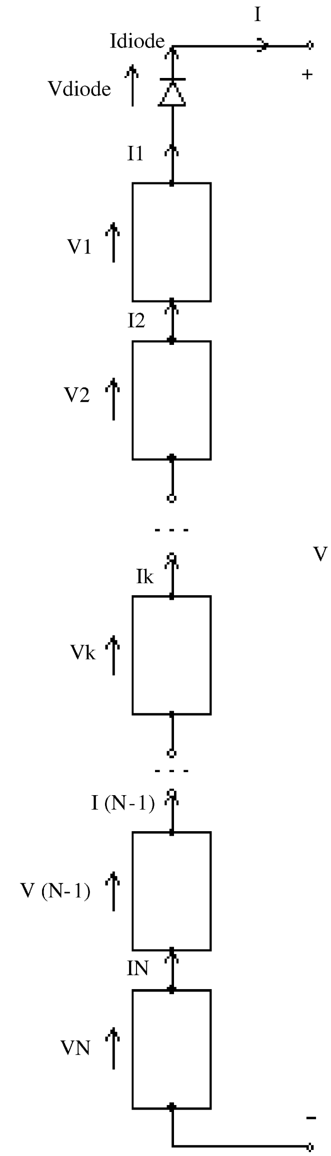

Fig. 2. String of N PV panels connected in series and including the blocking diode.

matrices [10].

$$J = \begin{pmatrix} 1 & 1 & 1 & \dots & 1 & \dots & 1 & 1 & 1 \\ \frac{\partial I_1}{\partial V_1} & -\frac{\partial I_2}{\partial V_2} & & & & & & & \\ \frac{\partial I_1}{\partial V_1} & & -\frac{\partial I_3}{\partial V_3} & & & & & 0 & \\ \vdots & & & \ddots & & & & & \\ \frac{\partial I_1}{\partial V_1} & & & & -\frac{\partial I_k}{\partial V_k} & & & & \\ \vdots & & & & & \ddots & & & \\ \frac{\partial I_1}{\partial V_1} & & 0 & & & & -\frac{\partial I_{N-1}}{\partial V_{N-1}} & & \\ \frac{\partial I_1}{\partial V_1} & & & & & & & -\frac{\partial I_N}{\partial V_N} & \\ \frac{\partial I_1}{\partial V_1} & & & & & & & & -\frac{\partial I_{\text{diode}}}{\partial V_{\text{diode}}} \end{pmatrix} \tag{12}$$

Moreover, the first row is composed by $(N+1)$ constants, while all the other rows require the evaluation of $\mathrm{d}I_1/\mathrm{d}V_1$ and the calculation of just another derivative. As a whole, the evaluation of the system (11) requires N times the use of Eq. (6) and one time Eq. (1) referring to the blocking diode; the calculation of the Jacobian matrix requires N evaluations of Eq. (10) and one evaluation of Eq. (13).

$$\frac{\partial I_{\text{diode}}}{\partial V_{\text{diode}}} = -\frac{I_{\text{sat,diode}}}{V_{t,\text{diode}}} \mathrm{e}^{-V_{\text{diode}}/V_{t,\text{diode}}}. \tag{13}$$

Such features are useful both in terms of memory requirements during the simulation and of computation time.

In Section 3, the features of the method are described by means of a numeric example.

3. Simulation results

Simulations have been conducted by considering Kyocera KC120 PV panels, characterized by 36 series connected cells; the area of each cell is equal to $0.0225\,\mathrm{m}^2$ while $R_s = 0.006\,\Omega$ and $R_h = 10^4\,\Omega$.

A string with two PV panels connected in series, and with the blocking diode has been simulated. In this case the order of the system is 3. The panels have been considered identical in terms of manufacturing parameters and working temperature ($T = 320\,\mathrm{K}$).

On the other hand, their irradiation level has been considered very different, namely $S = 1000\,\mathrm{W/m}^2$ for the first panel and $S = 100\,\mathrm{W/m}^2$ for the second one.

The whole simulation has been conducted in Matlab® environment; it required 45.3 s (on an Intel Centrino 2.0 GHz platform) in order to calculate 100 linearly spaced points of the power–voltage characteristic of the PV array. The samples of the current in the series and of the voltage distribution over the three devices have been also stored during simulation. The curves are reported in Figs. 3 and 4. They put in evidence the effect of the panel that receives the lower irradiance level in terms of string current drop at high voltage values.

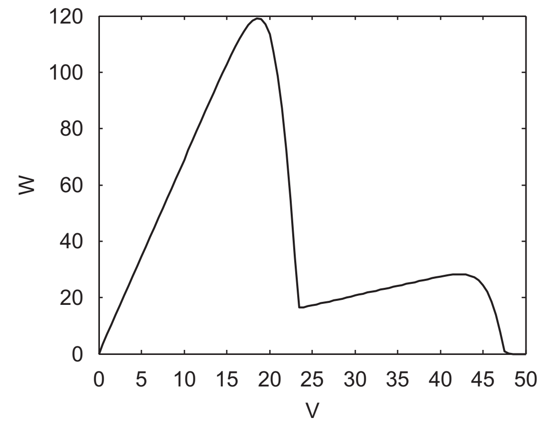

Fig. 3. Power [W] versus voltage [V] characteristic of the simulated mismatched PV field.

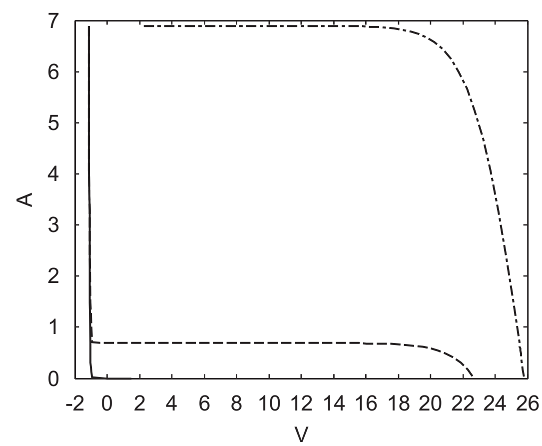

Fig. 4. Current [A] versus voltage [V] characteristic of the three devices in the simulated string. Continuous line = blocking diode curve, dashed line = curve of the panel with irradiation $S = 100\,\mathrm{W/m}^2$, dash-dotted line = curve of the panel with irradiation $S = 1000\,\mathrm{W/m}^2$.

It is worth noting that the curve of Fig. 3, obtained under mismatching conditions of the PV string, exhibits two maxima at two different voltage levels, with that one occurring at about 44 V being characterised by a consistently lower value of the power with respect to the other one placed at about 18 V. This occurrence can compromise the energy conversion operated by the switching converter connected at the string terminals and responsible for the MPPT. This can be understood by comparing plots of Fig. 3, representing the mismatched string, with that one of Fig. 5, obtained by imposing a unique irradiance level $S = 1000\,\mathrm{W/m}^2$ for both the panels. If the MPPT controller acts so that the string works at about 40 V under uniform irradiance, it ensures that the maximum power—about 260 W—is converted. If a sudden irradiance drop (from $S = 1000$ to $100\,\mathrm{W/m}^2$) occurs on one panel and the MPPT algorithm is not able to perform a ''global search'' of the

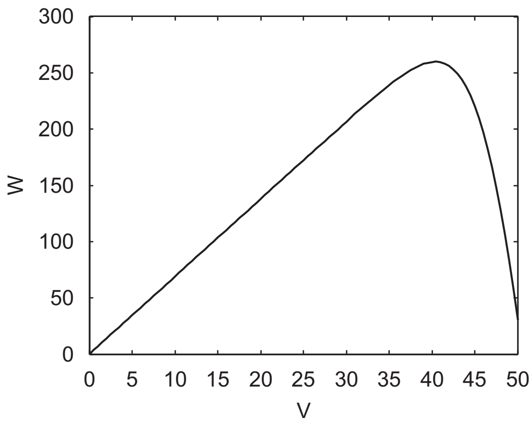

Fig. 5. Power versus voltage characteristic of the simulated matched PV field.

new maximum power point, the relative maximum placed at about 40 V (see Fig. 3) is the likely new operating point. This means that the MPPT controller is not able to track the real maximum power point and that about 90 W (the difference between the maximum power of the best operating point at about 18 V and the power of an operating point placed at about 44 V) are wasted due to MPPT algorithm limit.

Such considerations have been verified by means of a PSIM® simulation of the PV field controlled by means of a boost switching converter that performs the MPPT function and matches the PV field with a 48 V battery (see Fig. 6). The layout puts in evidence two dynamic link libraries that implement the PV field (on the left side) and the P & O based MPPT controller (at the bottom). In

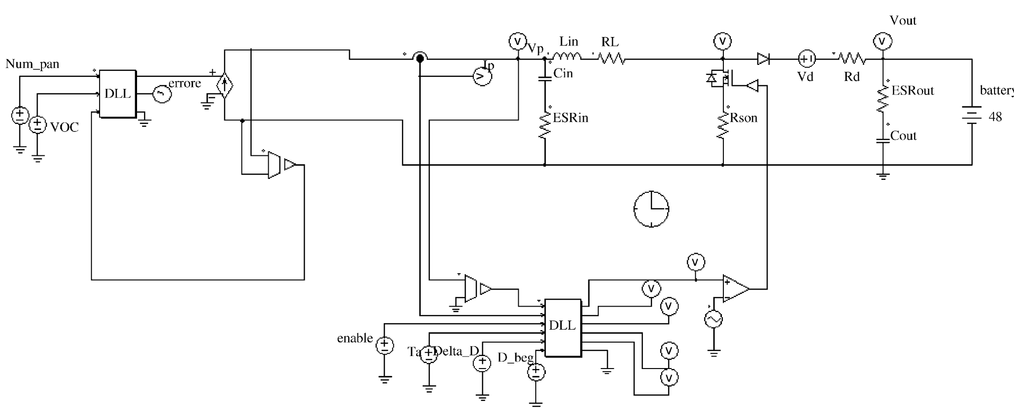

Fig. 6. PSIM schematics. Lin = 273 μH, RL = 0.2 Ω, Cin = 6.5 μF, ESRin = 13 mΩ, Rson = 13 mΩ, Vd = 1.06 V, Rd = 177 mΩ, Cout = 13 μF, ESRout = 6.2 mΩ.

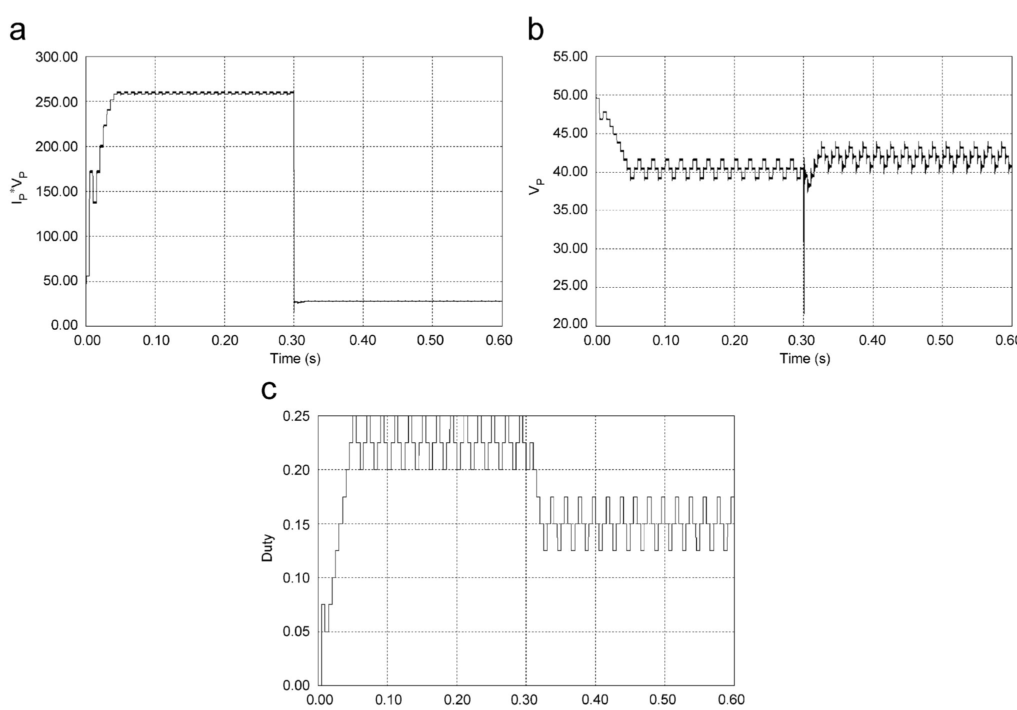

Fig. 7. MPPT during a solar irradiation drop at $t = 0.3$ s. (a) PV array output power, (b) PV array voltage, (c) boost converter duty cycle.

particular, the case of a sun irradiance drop involving one of the two panels of the array has been simulated: the steep transition between the characteristic of Fig. 5 and that one of Fig. 3 occurs at $t = 0.3\,\mathrm{s}$ (see Fig. 7). The P & O controller tracks the lower maximum because the voltage at which it occurs (see Fig. 7b) is close to the voltage corresponding to the unique maximum of the characteristic depicted in Fig. 5. Fig. 7 also puts in evidence the three-points behaviour at both steady states: this aspect characterizes the hill climbing of the two maximum power points tracked in correspondence of the two different operating conditions. This result is confirmed by the boost converter duty cycle variation shown in Fig. 7c.

4. Conclusions and future work

In this paper a non- linear model of mismatched PV fields is introduced. It allows to simulate heterogeneous arrays, with subsections (cells, groups of cells, panels or groups of panels) characterized by different irradiation levels, temperatures, semiconductor materials, areas, operating parameters and so on. The model also allows to take into account manufacturing tolerances and drifts ascribable to aging effects.

Further work is in progress in order to use the simulator for the development of a MPPT strategy that would be able to ensure an efficient power conversion even when the PV field works in mismatched conditions.

Acknowledgements

The research activities whose results are described in this paper have been supported by University of Salerno and MIUR PRIN 2006 funds.

References

[1] E.L. Meyer, E. Ernest van Dyk, The effect of reduced shunt resistance and shading on photovoltaic module performance, in: Conference Record of the Thirty-first IEEE Photovoltaic Specialists Conference, 2005, 3–7 January 2005, pp. 1331–1334.
[2] N.D. Kaushika, N.K. Gautam, IEEE Trans. Energy Convers. 18 (1) (2003) 127.
[3] R. Bruendlinger, B. Bletterie, M. Milde, H. Oldenkamp, Maximum power point tracking performance under partially shaded PV array conditions, in: Proceedings of the Twenty-first European Photovoltaic Solar Energy Conference, Dresden, Germany, 4–8 September 2006, pp. 2157–2160.
[4] T. Oozeki, K. Otani, K. Kurokawa, Accuracy of estimated shading loss ratio by means of SV method—an extraction algorithm of maximum pattern, in: Conference Record of the Thirty-first IEEE Photovoltaic Specialists Conference, 2005, 3–7 January 2005, pp. 1804–1807.
[5] C.E. Chamberlin, P. Lehman, J. Zoellick, G. Pauletto, Sol. Energy 54 (3) (1995) 165.
[6] http://mathworld.wolfram.com/LambertW-Function.html.
[7] A. Jain, S. Sharma, A. Kapoor, Sol. Energy Mater. Sol. Cells 90 (2006) 25.
[8] S. Liu, R.A. Dougal, IEEE Trans. Energy Convers. 17 (2) (2002) 285.
[9] V. Quaschning, R. Hanitsch, Sol. Energy 56 (6) (1996) 513.
[10] W.H. Press, Numerical Recipes in C, The Art of Scientific Computing, second ed., Cambridge University Press, 2002.